Detonation propagation in a semi-confined mixture with a diffuse interface

Michael McLoughlin, Vahid Yousefi Asli and Gaby Ciccarelli
Queen's University
Kingston, Ontario, Canada

1 Introduction

The study of detonation wave propagation through a semi-confined reactive gas mixture is of interest for industrial explosion safety [1] and the development of detonation-based propulsion system. The interface between the reactive mixture and an inert gas is either sharp or diffuse, depending on if a thin film initially separates the two gases. For either condition, a detonation wave travels through the reactive layer and the lateral expansion of the products drives an oblique shock in the inert gas layer. For the diffuse interface, mixture dilution at the interface results in detonation wave curvature within the layer. For a sharp interface, Rudy et al. [2] reported a critical propagation layer thickness for stoichiometric hydrogen-oxygen of three detonation cells. The thin film separation prevents the mixing of gas across the boundary but also provides some level of confinement that can affect detonation propagation. The measurement of the critical height without a separation film is much more problematic because there is no unique cell size [3]. In these experiments, the composition gradient across the interface is difficult to control, and to characterize.

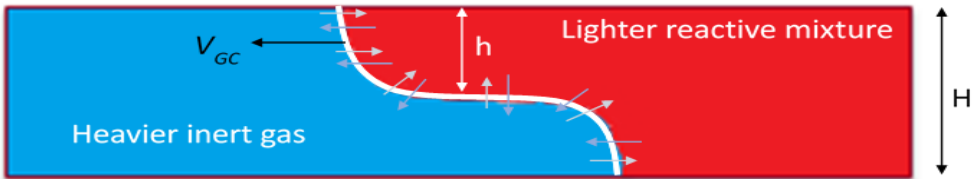

Figure 1: Schematic showing gravity current producing a layer thickness h in a channel of height H.

Lieberman et al. [4] performed a unique experiment where a gravity current, generated by lifting a gate initially separating a combustible mixture and an inert gas, was used to produce a stratified layer in a 150 mm tall channel, see Fig. 1. The main objective of the study was to characterize the effect of the diffuse interface on the structure of the detonation wave visualized by schlieren photography. Specifically, they proposed that the decoupling of the detonation corresponds to the location where a dramatic change in the induction zone length (calculated based on an assumed local composition profile) occurred. Bauwens and Dorofeev proposed a general detonation propagation failure criterion governed by the distribution of the cell size. This criterion proposes a limit for the propagation of a planar detonation wherein the increase in cell size cannot increase by more than 10% over a distance equal to the cell size ($d\lambda/dx<0.1$), as well as the layer accommodating at least a minimum number of 5-10 cells [5]. More recently, Metrow et al. [6] performed similar gravity current driven layer (hydrogen/oxygen over argon) experiments in a narrow

channel, with high-speed video to capture detonation wave propagation and simultaneous soot foils to capture the cellular structure. The evolution of the gravity current was simulated by CFD in order to get the argon distribution that was used to calculate the cell size distribution throughout the layer. Applying the criterion directly to the breakdown in the cell structure showed good agreement along the horizontal interface but not at the leading edge of the layer. Melguizo et al. [7] applied this criterion to the numerical simulation of the Lieberman et al. experiments. They proposed that the failure criterion is conservative, they showed that the detonation cell structure breaks down at $d\lambda/dx$ of roughly 0.5.

The failure of the Bauwens-Dorofeev criteria to predict the breakdown of the cell structure at the layer leading edge in [5] was attributed to the non-ideal change in channel width at the door, possibly leading to turbulent mixing during door opening. In this study, the door opening and channel width, before and after the door, are the same 12.7 mm. The objective of this study is to capture the detonation failure using video and soot foils and to evaluate the Bauwens-Dorofeev failure criteria.

2 Experimental

The apparatus is comprised of six 0.61 m long sections; the first four sections serve the purpose of generating a detonation wave via flame acceleration. A flame is ignited by a spark plug located at the endplate and fence type obstacles, mounted on the top and bottom plates equally spaced at 76 mm, in the first three sections are used to promote flame acceleration and deflagration-to-detonation transition (DDT). The obstacle blockage ratios in sections 1, 2, and 3, are 66%, 50%, 33%, respectively. The fourth section has no obstacles, so the detonation wave can stabilize before entering the optical test-section. Four ion probes mounted on the top channel wall of the third and fourth sections, equally spaced 0.3 m apart provide combustion front time-of-arrival data used to obtain the combustion front velocity. The test-section is isolated from the predetonator (first four sections) by a manually operated sliding door that has an aperture similar to the channel inner cross-section of 63.5 mm by 12.7 mm. The predetonator is filled with hydrogen/oxygen and the test section and dump tank are filled with argon to 1 atmosphere. The sliding door is opened, and after a pre-set delay the ignition system is activated. This delay time is the main parameter in the experiment as it governs how far into the test section the hydrogen/oxygen gravity driven layer develops by the time the detonation wave arrives.

The effect of the premixed predetonator reactivity was investigated by varying the H2-O2 equivalence ratio (ER) from 1.0 to 2.5. To keep the layer velocity constant, the density of the predetonator mixture was kept constant by adding a proportional amount of nitrogen. Both diluting the predetonator mixture with nitrogen and increasing the ER reduce the mixture reactivity and increase the detonation cell size. The rate of argon diffusion into the layer is not expected to change much because hydrogen is the minor component and the diffusivity of argon into nitrogen and oxygen is very similar.

2 Results and Discussion

Schlieren video images showing detonation propagation through the layer that develops over argon, for three predetonator H2-O2 equivalence ratios (ERs), with a delay of 1.5 s is shown in Fig. 2a-c. The schlieren system is not sensitive enough to see the layer thickness in these images, but it lies roughly at half the height of the field-of-view (FOV). For the ER=1.0 and 2.0 (images in Fig. 2a and 2b), the detonation wave structure is similar, it is curved in the layer due to a vertical gradient in argon concentration. Since the triple-points and the transverse waves are very closely spaced (cell size about 1 mm), they can barely be made out in the images. Below the layer, the detonation decouples into an inert oblique shock followed by a turbulent contact surface, as denoted in Fig. 2d, that separates the hot combustion products and the shock compressed argon. The oblique shock interacts with the bottom wall (6 mm outside the FOV) forming a reflected shock that propagates in the products. A slightly thicker reaction zone in the layer and larger scale perturbations along the contact surface are observed for the ER=2.0 images in Fig. 2b, due to the larger detonation cell size in the layer. In the bottom images it can be observed that the detonation decouples slightly sooner in the channel for the ER=2.0 predetonator. On the other hand, the detonation for the ER=2.5 predetonator starts to decouple almost immediately upon entering the FOV. Note the detonation propagates in the upstream part of the layer that extends back into the predetonator section 4 (before the FOV in Fig.

2). A hot spot and detonation kernel forms at the leading edge in Fig. 2c image 2, but it does not successfully reinitiate the detonation wave as it completely decouples in image 5.

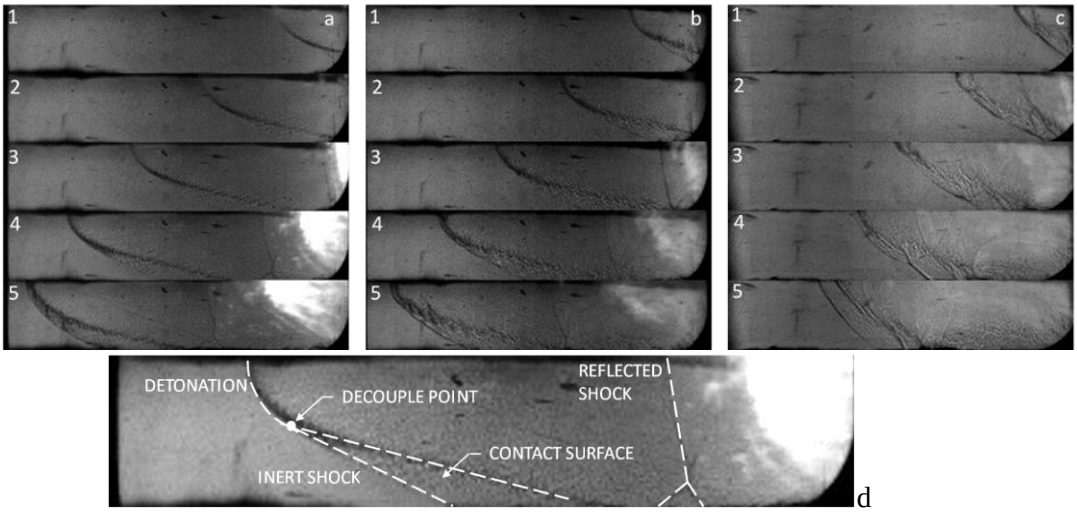

Figure 2 Schlieren video frames of detonation propagation for different hydrogen-oxygen predetonator mixtures into argon for 1.5 s delay: a) ER=1.0, b) ER=2.0, c) ER=2.5, d) detonation structure highlights

Figure 3 gives the detonation front velocity as a function of the distance obtained from the high-speed video for H2-O2 into argon for a 1.5 s delay. The extent of the FOV is indicated by the vertical black dotted lines, and the CJ velocity for ER=1.0 and 2.0 (no argon dilution) is shown. For ER between 1.0 and 2.0, the detonation speed drops steadily until just before the end of the FOV and then drops off suddenly at the point of decoupling; note the shock velocity is plotted for the failing wave, not the flame velocity. The chaotic nature of the propagation for the higher ER layers is highlighted in the plot by connecting the data points with lines as the velocity varies wildly between frames. The detonation does not ever propagate steadily and features two main re-initiations, the second of these initiations just after 225 mm corresponds to the images in Fig. 2c. This propagation limit of ER=2.5 aligns with the findings in Metrow et al. [6]. For ER=2.25, the detonation enters the FOV very unsteady, recovering momentarily before decoupling again and then failing. This "chugging" is typical of detonation propagation near the propagation limit.

The soot foil imprint obtained for a test with stoichiometric hydrogen-oxygen into argon, for a 1.5 s delay, is provided in Fig. 4. The cell-filled region is tapered, consistent with the expected shape of the layer. Most of the layer generated very small detonation cells of about 1 mm. The size of the cells along the bottom interface are noticeably larger. The lowest triple-points have no opposing triple-point (moving upwards) to interact with, so they trail off as vertical wispy streaks, see Fig. 4b. The cell size progressively increases at the layer leading-edge, indicating high amounts of argon dilution that eventually result in the detonation decoupling into a shock wave followed by a flame, as observed in Fig. 2a, image 5. When the detonation fails, the triple-points weaken in strength and the trajectory lines fade in strength. Experiments were also carried out with nitrogen initially in the test section, schlieren videos and soot foil imprints are not presented due to space limitations.

Numerical modeling of the flow, including the complex flow generated during the 0.2 s door opening, provided the time evolution of the non-uniform composition in the channel. Three-dimensional simulations were carried out with ANSYS Fluent version 18, including viscosity and multi-component mass diffusion, details can be found in [6]. The predicted CJ velocity along the top wall corresponding to the simulation for a predetonator ER of 1.0 into argon is plotted in Fig. 3. The calculated CJ detonation velocity follows a similar slow deceleration as the measured velocity up to approximately 225 mm. Beyond this axial position, the velocity decreases sharply as the leading edge of the layer is reached. Figure 3 shows that the detonation fails before the end of the layer. The lower velocity before failure is due to viscous losses that are not accounted for in the calculation of the CJ velocity profile.

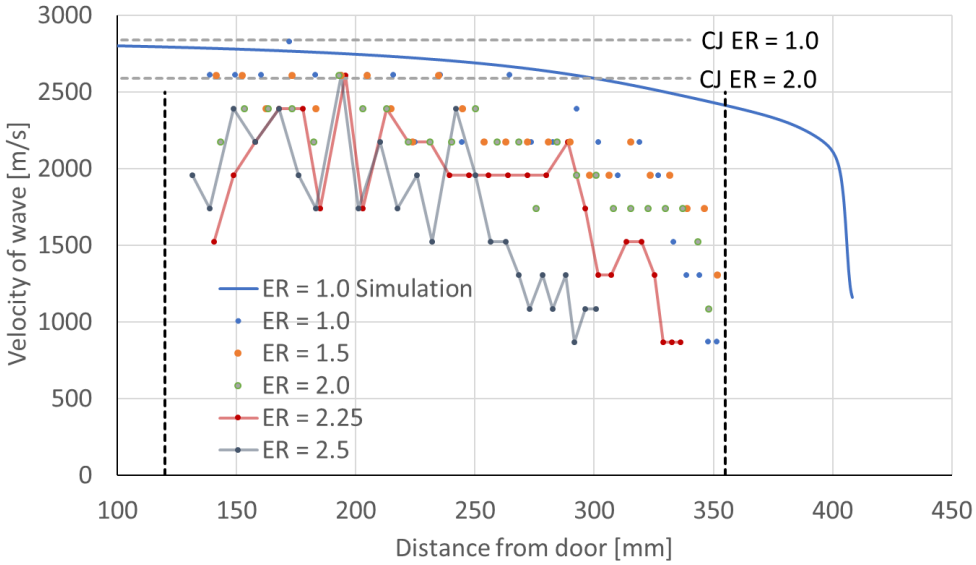

Figure 3: Velocity of the detonation front for different predetonator hydrogen-oxygen ERs into argon. All tests correspond to a 1.5 s delay. Vertical lines represent the edge of the camera FOV.

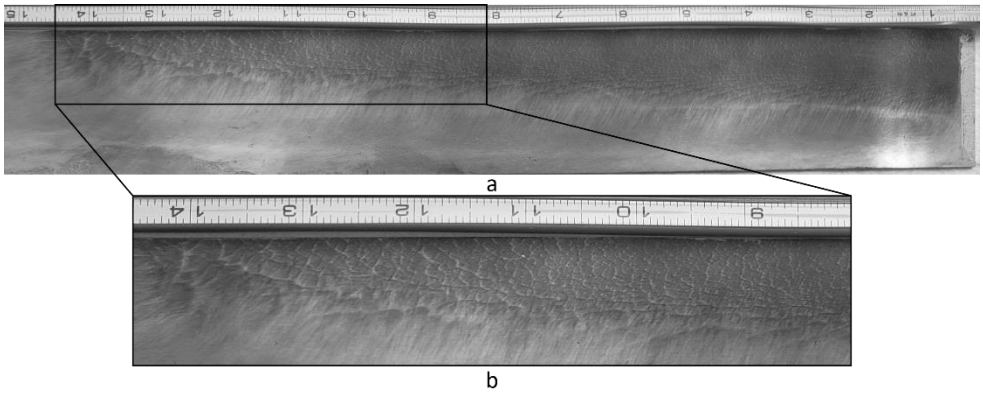

Figure 4. a) Soot foil for ER=1 into argon, b) magnification of rectangle area in Fig. 4a. Ruler shows inches.

The decoupling of the detonation before the end of the layer was detected by three different approaches: 1) end of the cell structure on the soot foil, 2) separation of the detonation into a shock and flame on the schlieren video, 3) sudden drop in the reaction front velocity measured from video taken of the foil soot incandescence. The propagation distance was measured from the downstream edge of the door, located 96 mm upstream of the right-edge of the foil. The measured detonation propagation distance obtained from the three approaches are provided in Fig. 4. The data points from the soot foil cell structure and the soot incandescence video are from the same tests, as a result the data point pairs are in very close agreement. The schlieren and soot foil based data, obtained from different tests, also show excellent agreement. For delay times less than 1.5 s, the measured detonation propagation distance increases roughly linearly. The position of the layer leading edge up to 2 ms (from the simulations) is also provided in Fig. 4. For argon, the detonation fails just short of the layer leading edge, whereas, for nitrogen, the detonation fails well before the layer leading edge. The detonation propagation distance asymptotes to roughly 550 mm for the argon and 275 mm for the nitrogen. These results show that there is a critical time for diffusion of the inert gas into the leading edge of the layer that limits the length of the detonable part of the layer. This is an important finding with respect to explosion safety because gravity driven layers of this type become self-limiting in terms of the extent of the detonable cloud. In an accident scenario where air, that contains 79% nitrogen, is the surrounding atmosphere, this can severely limit the detonable region.

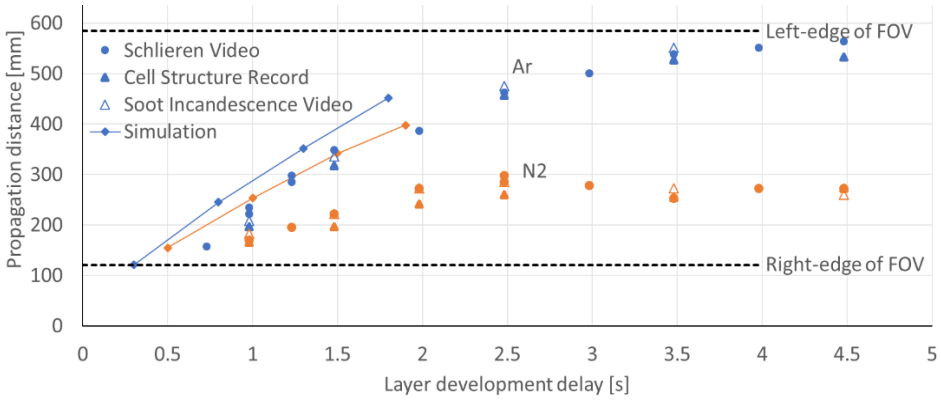

Figure 4. Detonation propagation distance for a stoichiometric hydrogen-oxygen predetonator into argon (blue) and nitrogen (orange) and the CFD predicted leading edge of the layer (solid line).

The CFD midplane argon distribution and the soot foil imprint are overlaid in Fig. 5 for tests with 2.5 s delay, for hydrogen-oxygen ER=1.0 and 2.0 predetonators into argon. Argon diffusion into these mixtures is not expected to be different, so the argon distribution obtained for ER=1.0 was used in both. The detonation failure criterion used by Lieberman et al. [4] is a rapid increase in the calculated ZND induction zone length. The Shock and Detonation Tool Box [8] was used to calculate the ZND induction zone length. For hydrogen-oxygen, this corresponds to 70% and 50% argon dilution for ER of 1.0 and 2.0, respectively. The yellow contour (70% argon) does a good job of predicting the lower bound of the cell structure in Fig. 5a, and the green contour (50% argon) does the same in Fig. 5b for the ER=2.0 predetonator. However, the detonation fails much earlier in the axial direction compared to that predicted by this basic criterion, especially for the ER=1.0 predetonator.

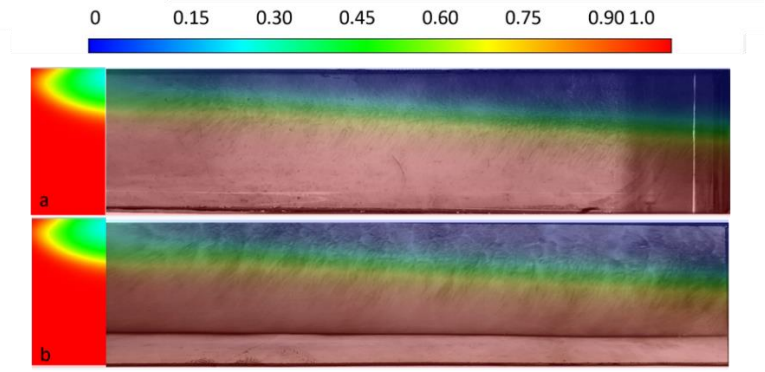

Figure 5. Overlays of the midplane simulation argon mole fraction over the soot foil impression obtained for a hydrogen-oxygen predetonator of ER=1.0 (a) and 2.0 (b) into argon for a delay time of 1.5 s.

The Bauwens and Dorofeev detonation failure criterion [5] requires the cell size distribution through the layer based on the local argon mole fraction. Cell size data for argon diluted hydrogen-oxygen from the CalTech Detonation database was used to establish a $\lambda=A\Delta$ linear fit, and the fit was used to generate the cell size distribution. The curves shown in Fig. 6 correspond to the criterion ($d\lambda/dx=0.1$) evaluated at the midplane and back wall where the foil was located. The curves overlap at the bottom of the layer but the curve extends further axially on the midplane than at the walls due to viscous effects that slow the advancement of the layer. The $d\lambda/dx=0.1$ criterion corresponds to where the detonation cell size starts to get larger at the bottom of the layer. However, the failure at the leading edge occurs slightly before the wall $d\lambda/dx=0.1$ critical value. Note, the $d\lambda/dx=0.5$ curve proposed in [7] would lie beyond the $d\lambda/dx=0.1$. The last full detonation cell occurs at an axial position that corresponds to about five cells across the layer height, so detonation failure in the axial direction is consistent with the minimum required 5-10 cells [5].

The larger cells seen on the foil in Fig. 6b for nitrogen are the result of the stronger dilution effect of the diatomic molecule. The cell structure ends well before the tip of the dλ/dx=0.1 curve, but the layer is very thin at that point so the 5-10 cell requirement is not met. This stronger dilution effect also results in a shorter axial propagation distance, as discussed in reference to Fig. 4; the maximum propagation distance for nitrogen is significantly shorter than that for argon.

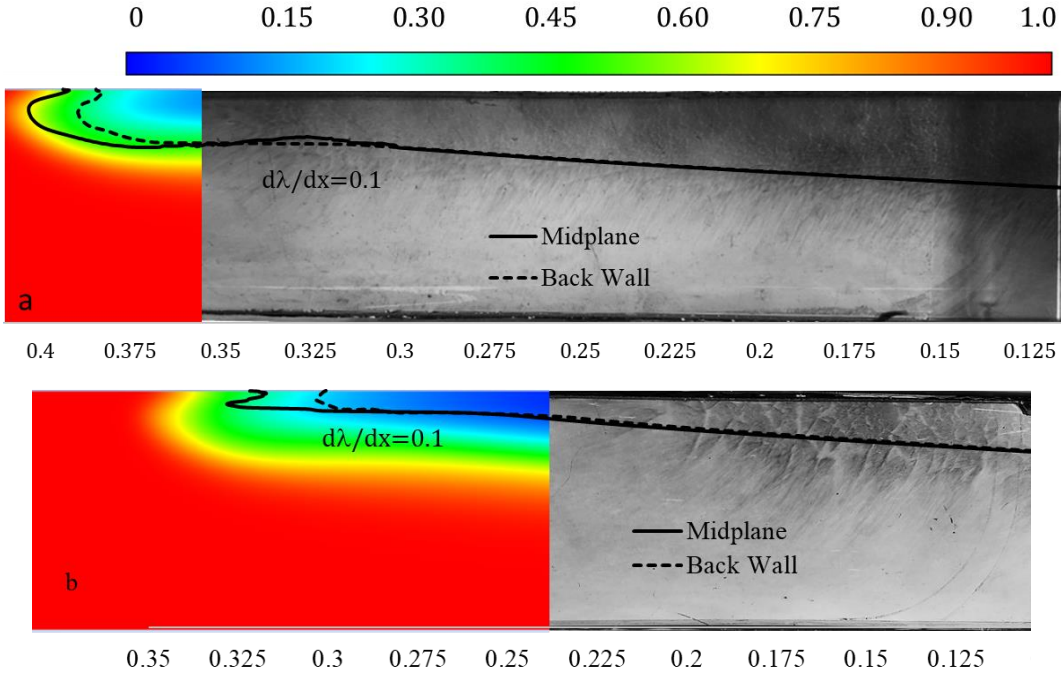

Figure 6. Overlay showing the back wall simulation diluent mole fraction contours at the layer leading edge, the dλ/dx=0.1 curve deduced from the mole fraction distribution at the midplane and back wall, and the soot foil impression obtained for stoichiometric hydrogen-oxygen with 1.5 s delay.

3. Conclusions

The study showed that detonation propagation through a gravity-driven combustible layer is self-limiting due to over-mixing at the layer leading edge driven by mass transport of the surrounding inert gas. CFD simulations successfully predicted the layer diluent (argon and nitrogen) distribution based on a comparison with the recorded cell structure. The CFD results were used to show that the detonation failure criterion proposed in [5] successfully predicts the extent of detonation propagation in the layer.

References

1. M. Kuznetsov, J. Yanez, J. Grune, A. Freidrich and T. Jordan, Hydrogen combustion in a flat semi-confined layer with respect to the Fukushima Daiichi accident, Nuclear Engineering and Design, 286:36-48, 2015.
2. W. Rudy, M. Kuznetsov, R. Porowski, A. Teodorczyk, J. Grune and K. Sempert, Critical conditions of hydrogen-air detonation in partially confined geometry, Proc. of the Combust. Inst., 34(2):1965-1972, 2013.
3. J. Grune, K. Sempert, A. Friedrich, M. Kuznetsov and T. Jordan, Detonation wave propagation in semi-confined layers of hydrogen–air and hydrogen–oxygen mixtures, I. J. Hydrogen Energy, 42 (11): 7589-7599, 2017.
4. D. H. Lieberman and J. E. Shepherd, Detonation interaction with a diffuse interface and subsequent chemical reaction, Shock Waves, 16: 421-429, 2007.
5. C. R. L. Bauwens and S. B. Dorofeev, Modeling detonation limits for arbitrary non-uniform concentration distributions in fuel–air mixtures, Combustion and Flame, 221:338-345, 2020.
6. C. Metrow, V. Yousefi Asli Mozhdehe and G. Ciccarelli, Detonation Propagation across a stratified layer with a diffuse interface, in the 38th International Symposium on Combustion presentation, Adelaide, 2021.
7. J. Melguizo-Gavilanes, M. Peswani and B. M. Maxwell, Detonation-diffuse interface interactions: failure, reiniation, and propagation limits, Proc. of the Combust. Inst., 38(3): 3717-3724, 2021.
8. SD Tool Box downloaded from https://shepherd.caltech.edu/EDL/PublicResources/sdt/